Reactivity of the Molecular Hydrogen Complex $[IrH_4(PMe_2Ph)_3]BF_4$ toward Olefins. The Origin of Stereochemical Rigidity of $M(PR_3)_3(olefin)_2$ Species

Eric G. Lundquist,[1a] Kirsten Folting,[1a] William E. Streib,[1a] John C. Huffman,[1a] Odile Eisenstein,*[1b] and Kenneth G. Caulton*[1a]

Contribution from the Department of Chemistry and Molecular Structure Center, Indiana University, Bloomington, Indiana 47405, and Laboratoire de Chimie Theorique, Batiment 490, Centre de Paris-Sud, 91450 Orsay, France. *Received June 12, 1989*

Abstract: Stoichiometric protonation of IrH_3P_3 (P = PMe_2Ph) with HBF_4 in CH_2Cl_2 leads to the formation of $IrH_4P_3^+$. T_1 measurements along with reactivity studies suggest that this complex contains two hydride ligands and a coordinated dihydrogen molecule. Since H_2 is easily lost from this species, $IrH_4P_3^+$ serves as a convenient precursor to the highly reactive, unsaturated hydride species $IrH_2P_3^+$. $IrH_4P_3^+$ reacts with ethylene to initially form the hydrido–ethylene complex *cis,mer*-$IrH_2(C_2H_4)P_3^+$. Labeling studies on this complex indicate the existence of a hydrido–ethyl equilibrium partner. Added ethylene promotes the reductive elimination of ethane and produces the nonfluxional bis-ethylene complex $Ir(C_2H_4)_2P_3^+$, which was structurally characterized. $Ir(C_2H_4)_2P_3^+$ was found to exchange with labeled C_2H_4, thus indicating the existence of the monoethylene species $Ir(C_2H_4)P_3^+$. This species can be trapped with added ligands (MeCN or CH_3^-) and reacts with H_2 to regenerate $IrH_2(C_2H_4)P_3^+$, thus closing the catalytic cycle for ethylene hydrogenation. Allene reacts with $IrH_4P_3^+$ to produce propene and initially an unsymmetrical bis-allene complex which undergoes a slow isomerization to the symmetrical bis-allene complex. $Ir(C_3H_4)_2P_3^+$ was structurally characterized and shown to contain two uncoupled allene ligands. EHT calculations done on the model compound $Ir(C_2H_4)_2(PH_3)_3^+$ give a high barrier for rotation of one (or two) olefin(s) as well as a high barrier for pseudorotation. The origin of these high-energy barriers stems from the absence of π-acceptor ligands such as CO on the metal. The unsymmetrical bis-allene isomer is calculated to be slightly less stable than the symmetrical one. The stereochemical rigidity of the bis-allene and bis-ethylene complexes is due to the same causes. Crystallographic data for $[Ir(C_2H_4)_2(PMe_2Ph)_3]BF_4 \cdot 0.5H_2O$: a = 10.580 (5) Å, b = 20.332 (12) Å, c = 27.771 (17) Å, β = 93.84 (3)° with Z = 8 in space group $P2_1/c$. For $[Ir(C_3H_4)_2(PMe_2Ph)_3]BF_4$: a = 21.817 (7) Å, b = 13.999 (2) Å, c = 10.022 (1) Å, β = 92.91 (1)° with Z = 4 in space group $P2_1/a$.

Facile loss of coordinated H_2 is a common characteristic of certain dihydrogen (η^2-H_2) complexes.[2] In the event that an η^2-H_2 complex also contains hydride ligands, this characteristic of η^2-H_2 to serve as a good leaving group presents a convenient opportunity to access, under exceptionally mild conditions, the currently rare field of unsaturated hydride complexes.

We report here on the protonation of *fac*-$IrH_3(PMe_2Ph)_3$ with $HBF_4 \cdot OEt_2$ to produce the cationic complex $IrH_4P_3^+$,[3] which is shown to contain intact H_2 but also serves as a ready source of the unsaturated hydride transient $IrH_2P_3^+$.[4] The reactivity of this species toward olefins is the subject of the present report.

Experimental Section

All manipulations were carried out by using standard Schlenk and glovebox procedures under prepurified nitrogen or vacuum. Solvents (THF, benzene, toluene, pentane) were dried and deoxygenated by Na/K benzophenone and vacuum transferred prior to use. CD_2Cl_2 and CH_2Cl_2 were distilled from P_2O_5. CD_3CN was dried and distilled under N_2 from CaH_2. Methyl acrylate was purchased from Aldrich and used as received. The gases C_2H_4 (C.P. Grade, Matheson), allene (propa-1,2-diene) (Matheson), H_2 (Air Products), D_2 (C.P. Grade, 99.5%, Linde), and $^{13}C_2H_4$ (99% ^{13}C, Cambridge Isotope Laboratories) were used as received. ^1H, ^2H, ^{31}P, and ^{13}C NMR spectra were recorded on a Nicolet NT-360 spectrometer at 360, 55, 146, and 90 MHz, respectively. Proton T_1 values were determined at 200 K in CD_2Cl_2 (toluene-d_8 for *fac*-$H_3Ir(PMe_2Ph)_3$) by the inversion/recovery method at 360 MHz with a 180°-τ-90° pulse sequence. Where noted, precise quantities of gases were furnished by using a conventional calibrated gas manifold.

Synthesis of $[Ir(C_2H_4)_2(PMe_2Ph)_3]BF_4$. To a degassed 15-mL CH_2Cl_2 solution containing 150 mg (0.21 mmol) of $[IrH_4P_3]BF_4$ (generated in situ from H_3IrP_3 and $HBF_4 \cdot OEt_2$) was added excess (4 mmol) ethylene. Stirring this colorless solution for 1.5 h, followed by removal of solvent under vacuum, yielded a cream-colored powder in 97% yield: ^1H NMR (360 MHz, 25 °C, CD_2Cl_2) 1.35 (virtual triplet, J_{Me-P} = 3 Hz, 12 H), 2.05 (d, J_{Me-P} = 11 Hz, 6 H), 2.30 (br m, $CH_2{=}CH_2$, 4 H), 2.45 (br m, $CH_2{=}CH_2$, 4 H), 7.5–8.0 (m, P–Ph); $^{31}P\{^1H\}$ NMR (146 MHz, 24 °C, CD_2Cl_2) −42.0 (d, J_{P-P} = 22 Hz, 2 P), −55.5 (t, J_{P-P} = 22 Hz, 1 P); $^{13}C\{^1H\}$ NMR of $[Ir(^{13}C_2H_4)_2P_3]BF_4$ (90 MHz, 22 °C, CD_2Cl_2) 29.1 (d of d, $J_{^{13}C-^{13}C}$ = 44 Hz, $J_{^{13}C-P}$ = 5 Hz), 25.6 (d of d, $J_{^{13}C-^{13}C}$ = 44 Hz, $J_{^{13}C-P}$ = 12.5 Hz).

Synthesis of *cis,mer*-$[IrH_2(C_2H_4)(PMe_2Ph)_3]BF_4$. A 5-mm NMR tube containing 75 mg (0.11 mmol) of $[Ir(C_2H_4)_2P_3]BF_4$ was degassed and pressurized with excess H_2. After sealing and shaking the tube for 10 min, the ^1H NMR revealed total conversion to $IrH_2(C_2H_4)P_3^+$ and free ethylene: ^1H NMR (360 MHz, 20 °C, CD_2Cl_2) −12.00 (d of t, $J_{H-P_{trans}}$ = 93 Hz, $J_{H-P_{cis}}$ = 17 Hz, 1 H), −9.25 (d of t, $J_{H-P_{cis}} \approx J_{H-P_{cis}}$ = 14.5 Hz, 1 H), 1.00 (vt, J_{Me-P} = 3 Hz, 6 H), 1.30 (d, J_{Me-P} = 3 Hz, 6 H), 1.80 (vt, J_{Me-P} = 3 Hz, 6 H), 2.85 (s, $CH_2{=}CH_2$, 4 H), 7.0–8.0 (m, P–Ph); $^{31}P\{^1H\}$ (146 MHz, 24.0 °C, CD_2Cl_2) −35.6 (d, J_{P-P} = 19 Hz, 2 P), −50.6 (t, J_{P-P} = 19 Hz, 1 P); $^{13}C\{^1H\}$ NMR of $IrH_2(^{13}C_2H_4)P_3^+$ (90 MHz, 20 °C, CD_2Cl_2) 46.9 (s, $^{13}C_2H_4$). This product is also observed when the reaction of $IrH_4P_3^+$ with excess ethylene is monitored by ^1H NMR at −50 °C. No freezing out of the ethylene rotation is observed in either the ^1H or ^{13}C NMR spectra at this temperature.

Synthesis of $[Ir(C_3H_4)_2(PMe_2Ph)_3]BF_4$ (Thermodynamic Product). To a degassed 15-mL CH_2Cl_2 solution containing 175 mg (0.25 mmol) of $IrH_4P_3^+$ (generated in situ) was added excess allene (4 mmol). After stirring for 10 h, solvent and excess allene were removed under vacuum. The resulting white powder was washed with THF and filtered to give 180 mg of $[Ir(C_3H_4)_2P_3]BF_4$ (93% yield): ^1H NMR 360 MHz, 24 °C, CD_3CN) 1.30 (vt, J_{Me-P} = 4 Hz, 12 H), 1.65 (m, $C{=}CH_2$, 4 H), 1.73 (d, J_{Me-P} = 9 Hz, 6 H), 5.50 (d of m, J_{H-P} = 9 Hz, 2 H), 6.30 (d of m, J_{H-P} = 15.6, 2 H), 7.05 (m, P–Ph), 7.40 (m, P–Ph); $^{31}P\{^1H\}$ NMR (146 MHz, 24 °C, CD_2Cl_2) −46.4 (d, J_{P-P} = 17 Hz, 2 P), −59.0 (t, J_{P-P} = 17 Hz, 1 P); $^{13}C\{^1H\}$ NMR (90 MHz, 24 °C, CD_2Cl_2) 7.27 (d, J_{C-P} = 4.5 Hz (H-coupled, d of t, J_{C-P} = 4.5 Hz, J_{C-H} = 158 Hz), 10.21 (t, J_{Me-P}

(1) (a) Indiana University. (b) Orsay.
(2) (a) Kubas, G. J.; Unkefer, C. J.; Swanson, B. I.; Fukushima, E. *J. Am. Chem. Soc.* **1986**, *108*, 7000. (b) Crabtree, R. H.; Lavin, M.; Bonneviot, L. *J. Am. Chem. Soc.* **1986**, *108*, 4032. (c) Clark, H. C.; Hampden-Smith, M. *J. Am. Chem. Soc.* **1986**, *108*, 3829. (d) Morris, R. H.; Sawyer, J. F.; Shiralian, M.; Zubkowski, J. D. *J. Am. Chem. Soc.* **1985**, *107*, 5581. (e) Conroy-Lewis, F. M.; Simpson, S. J. *J. Chem. Soc., Chem. Commun.* **1986**, 506. (f) Crabtree, R. H.; Lavin, M. *J. Chem. Soc., Chem. Commun.* **1985**, 1661.
(3) Rhodes, L. F.; Caulton, K. G. *J. Am. Chem. Soc.* **1985**, *107*, 259.
(4) Lundquist, E. G.; Huffman, J. C.; Folting, K.; Caulton, K. G. *Angew. Chem., Int. Ed. Engl.* **1988**, *27*, 1165.

0002-7863/90/1512-855$02.50/0

Table I. Crystal Data for $[Ir(C_2H_4)_2(PMe_2Ph)_3]BF_4 \cdot 0.5H_2O$

empirical formula	$IrC_{28}H_{41}P_3BF_4 \cdot 0.5H_2O$
color	yellow
crystal dimensions (mm)	0.15 × 0.12 × 0.12
space group	$P2_1/c$
cell dimensions (at −155 °C)	
a =	10.580 (5) Å
b =	20.332 (12) Å
c =	27.771 (17) Å
β =	93.84 (3)°
molecules/cell	8
volume (Å^3)	5960.88
calcd density (g/cm^3)	1.671
wavelength (Å)	0.71069
molecular weight	749.58
linear absorption coeff (cm^{-1})	46.6
no. of unique intensities	7492
no. with $F > 0.0$	6790
no. with $F > 2.33\sigma(F)$	5950
R for averaging	0.071
final residuals	
$R(F)$	0.0693
$R_w(F)$	0.0645
goodness of fit for last cycle	1.20
max Δ/σ for last cycle	0.55

= 20 Hz) (H-coupled, q of t), 17.70 (d, J_{Me-P} = 32 Hz) (H-coupled, q of d), 103.3 (s), (H-coupled, t, J_{C-H} = 163 Hz), 127–132 (m, P–Ph), 149.2 (d of t, J_{C-P} = 18.1 Hz, J_{C-P} = 5 Hz) (H-coupled, no change).

Synthesis of $[Ir(C_3H_4)_2(PMe_2Ph)_3]BF_4$ (Kinetic Product). To a 5-mm NMR tube containing 80 mg (0.11 mmol) of $IrH_4P_3^+$ (generated in situ) in 0.4 mL of CD_2Cl_2 was added 0.20 mmol of allene. After 10 min, a ^1H NMR was recorded. This spectrum reveals the presence of propene (δ = 5.80 m (1 H), 4.85 m (2 H), 1.68 m (3 H)) and an iridium/allene complex. This complex can be isolated at this point by addition of pentane to the CD_2Cl_2 solution: ^1H NMR (360 MHz, 20 °C, CD_2Cl_2) 1.15 (vt, J_{Me-P} = 4 Hz, 6 H), 1.33 (vt, J_{Me-P} = 4 Hz, 6 H), 1.41 (m, $Ir(CH_2)$, 2 H), 1.80 (d, J_{Me-P} = 9 Hz, 6 H), 2.15 (m, $Ir(CH_2)$, 2 H), 5.00 (d of m, J_{H-P} = 10 Hz, J_{H-H} = 2 Hz, 1 H), 5.42 (m, J_{H-H} = 2 Hz, 1 H), 6.60 (m, J_{H-H} = 2 Hz, 1 H), 6.63 (d of m, J_{H-P} = 16 Hz, J_{H-H} = 2 Hz, 1 H), 7.0–7.60 (m, P–Ph); $^{31}P\{^1H\}$ NMR (146 MHz, 24 °C, CD_2Cl_2) −44.20 (d, J_{P-P} = 18 Hz, 2 P), −56.50 (t, J_{P-P} = 18 Hz, 1 P); $^{13}C\{^1H\}$ NMR (90 MHz, 10 °C, CD_2Cl_2) 9.10 (t, J_{Me-P} = 19 Hz), 9.20 (t, J_{Me-P} = 19 Hz), 11.0 (t of d, J_{C-P} = 17 Hz, J_{C-P} = 2 Hz), 11.5 (d, J_{C-P} = 8 Hz), 17.2 (d, J_{Me-P} = 31 Hz), 102.2 (d, J_{C-P} = 11 Hz), 104.3 (s), 150.7 (d of t, J_{C-P} = 16 Hz, J_{C-P} = 5 Hz), 154.8 (d of t, J_{C-P} = 7 Hz, J_{C-P} = 5 Hz).

Synthesis of $[Ir(C_2H_4)(CD_3CN)P_3]BF_4$. A 50-mg (0.07 mmol) sample of $[Ir(C_2H_4)_2P_3]BF_4$ is dissolved in CD_3CN. Gas evolution is observed, and ^1H NMR indicates total conversion to $Ir(C_2H_4)(CD_3CN)P_3^+$ within 30 min: ^1H NMR (360 MHz, 24 °C, CD_3CN) 0.87 (br m, $H_2C{=}CH_2$, 2 H), 1.25 (d, J_{Me-P} = 8 Hz, 6 H), 1.50 (m, $H_2C{=}CH_2$, 2 H), 1.60 (vt, J_{Me-P} = 4 Hz, 6 H), 1.85 (vt, J_{Me-P} = 4 Hz, 6 H), 7.0–7.8 (m, P–Ph); $^{31}P\{^1H\}$ NMR (146 MHz, 22 °C, CD_3CN) −38.3 (t, J_{P-P} = 20 Hz, 1 P), −42.9 (d, J_{P-P} = 20 Hz, 12 P); $^{13}C\{^1H\}$ NMR of $Ir(^{13}C_2H_4)(CD_3CN)P_3^+$ (90 MHz, 24 °C, CD_3CN) 21.7 (second-order AA′XX′ multiplet, see Figure 3).

Synthesis of $IrMe(C_2H_4)(PMe_2Ph)_3$. To a 100-mL Schlenk flask containing 80 mg (0.10 mmol) of $[Ir(C_2H_4)_2P_3]BF_4$ in 20 mL of THF was added 0.5 mL (1.4 M, 0.70 mmol) of MeLi in Et_2O at 0 °C. After stirring for 4 h, the reaction mixture was hydrolyzed with wet THF at 0 °C, and solvent was then removed under vacuum. This resulting yellow material was dissolved in C_6H_6 and filtered to remove Li salts. Removal of C_6H_6 gave pale yellow $IrMe(C_2H_4)P_3$; ^1H NMR (360 MHz, 22 °C, C_6D_6) 0.0 (t of d, J_{IrMe-P} = 9 Hz, J_{IrMe-P} = 4 Hz, 3 H), 1.00 (d, J_{Me-P} = 9 Hz, 6 H), 1.25 (m, $CH_2{=}CH_2$, 2 H), 1.43 (vt, J_{Me-P} = 3 Hz, 6 H), 1.60 (vt, J_{Me-P} = 3 Hz, 6 H), 1.70 (m, $CH_2{=}CH_2$, 2 H), 7.0–7.80 (m, P–Ph); $^{31}P\{^1H\}$ NMR (146 MHz, 23 °C, C_6D_6) −43.40 (t, J_{P-P} = 20 Hz, 1 P), −44.30 (d, J_{P-P} = 20 Hz, 2 P); $^{13}C\{^1H\}$ NMR obtained by using $IrMe(^{13}C_2H_4)P_3$ (90 MHz, 23 °C, C_6D_6) 22.7 (second-order AA′XX′ multiplet).

Synthesis of *mer*-$[Ir(H)CH_2CH_2C(O)OMe(PMe_2Ph)_3]BF_4$. To a 15-mL CH_2Cl_2 solution containing 200 mg (0.28 mmol) of $[IrH_4P_3]BF_4$ (generated in situ) was added 0.5 mL (5.5 mmol) of methyl acrylate. After stirring for 1 h, CH_2Cl_2 and excess methyl acrylate were removed under vacuum. Trituration with pentane/THF (10 mL) gave 208 mg (95% yield) of a white material: ^1H NMR (360 MHz, 24 °C, CD_2Cl_2) −27.75 (d of t, $J_{H-P_{cis}}$ = 11.8 Hz, $J_{H-P_{cis}}$ = 17.8 Hz, 1 H), 1.20 (m, Ir–CH_2, 2 H), 1.40 (overlapping vt, P–Me, 12 H), 1.50 (br d, P–Me, 6 H), 2.25 (m, CH_2–CO_2Me, 2 H), 3.65 (s, OMe, 3 H), 7.5–8.0 (m, P–Ph);

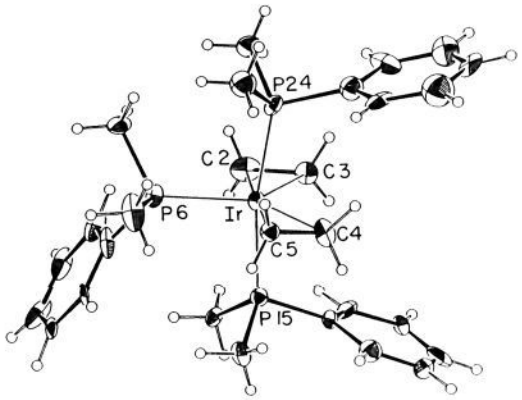

Figure 1. ORTEP drawing of $Ir(C_2H_4)_2(PMe_2Ph)_3^+$. Unlabeled ellipses are carbon; open circles are hydrogen.

$^{31}P\{^1H\}$ NMR (146 MHz, 24 °C, CD_2Cl_2) −21.0 (d, J_{P-P} = 19 Hz, 2 P), −34.0 (t, J_{P-P} = 19 Hz, 1 P); IR (Nujol mull) 2240 cm^{-1} (w, Ir–H), 1750 cm^{-1} (m, CO_2Me).

Reaction of $[Ir(C_3H_4)_2(PMe_2Ph)_3]BF_4$ with H_2. A 5-mm NMR tube containing 50 mg (0.065 mmol) of $[Ir(C_3H_4)_2(PMe_2Ph)_3]BF_4$ in CD_2Cl_2 was degassed and pressurized with an excess of H_2. ^1H NMR spectra recorded after 1 week revealed the presence of propane, $IrH_4P_3^+$, and unreacted $[Ir(C_3H_4)_2(PMe_2Ph)_3]BF_4$. After a total of 20 days, only $IrH_4P_3^+$ and propane were present as judged by ^1H NMR.

Reaction of $[Ir(C_2H_4)_2(PMe_2Ph)_3]BF_4$ with $^{13}C_2H_4$. To a 5-mm NMR tube containing 50 mg (0.065 mmol) of $[Ir(C_2H_4)_2P_3]BF_4$ in 0.5 mL of degassed CD_2Cl_2 was added 0.15 mmol of $^{13}C_2H_4$. After 30 min, ^1H NMR revealed the formation of $Ir(^{13}C_2H_4)_2P_3^+$ and unlabeled free ethylene.

Reaction of $[Ir(C_2H_4)_2(PMe_2Ph)_3]BF_4$ with D_2. A 5-mm NMR tube containing 60 mg (0.08 mmol) of $[Ir(C_2H_4)_2P_3]BF_4$ in 0.5 mL of CH_2Cl_2 was degassed and pressurized with an excess of D_2. After shaking for 20 min, the ^2H NMR was recorded: ^2H NMR (55 MHz, 22 °C, CH_2Cl_2) −11.59 (br d, $J_{^2H-P}$ = 15.5 Hz), −8.54 (br s), 2.40 (br s) of $IrD_2(C_2D_xH_{4-x})P_3^+$. A ^1H NMR (CH_2Cl_2) of this sample was obtained by using the Nicolet solvent saturation routine PRESAT. The observation of hydride resonances at −12.00 and −9.25 ppm, along with a resonance at 2.85 ppm, confirmed the presence of protons in these positions.

Reaction of $[IrH_2(C_2H_4)(PMe_2Ph)_3]BF_4$ with D_2. A 5-mm NMR tube containing 45 mg (0.062 mmol) of $[IrH_2(C_2H_4)(PMe_2Ph)_3]BF_4$ in degassed CD_2Cl_2 was pressurized with an excess of D_2. After shaking for 10 min, a ^2H NMR recorded: ^2H NMR (55 MHz, 22 °C, CH_2Cl_2) −11.60 (br d, $J_{^2H-P}$ = 15.5 Hz), −8.54 (br s), 2.40 (br s).

Crystallography of $[Ir(C_2H_4)_2(PMe_2Ph)_3]BF_4 \cdot 0.5H_2O$. A suitable fragment of a larger crystal grown by layering a CH_2Cl_2 solution with pentane and then cooling to −20 °C was cleaved under nitrogen and transferred to the goniostat by using standard inert atmosphere handling techniques and cooled to −155 °C for characterization and data collection.[5]

A systematic search of a limited hemisphere of reciprocal space located a set of diffraction maxima with symmetry and systematic absences corresponding to the unique monoclinic space group $P2_1/c$. Subsequent solution and refinement of the structure confirmed this choice. Characteristics of the data collection (6° ≤ 2θ ≤ 45°), processing, and refinement are given in Table I.

The structure was solved by a combination of direct methods (MULTAN78) and Fourier techniques. The unit cell contains two independent formula units, which have been designated "A" and "B"; the two independent cations show no statistically significant differences. A difference Fourier synthesis revealed the location of some, but not all, hydrogen atoms. All hydrogen atoms positions were therefore calculated by using idealized geometries and d(C–H) = 0.95 Å. These calculated positions were fixed for the final cycles of refinement.

A ψ scan of several peaks near χ = 90° indicated that absorption was less than 8%, so no correction was performed. A final difference Fourier was featureless, with the largest peaks being 1.58 and 1.45 e/Å^3, located in the vicinity of the Ir atoms. All other peaks were less than 1.0 e/Å^3. The results of the X-ray study are given in Tables II and III and Figure 1. The BF_4^- ions are unexceptional, B–F distances ranging from 1.33 (3) to 1.43 (3) Å with FBF angles from 102.5 (18) to 118.9 (24)°.

(5) For a general description of the diffractometer and crystallographic procedures, see: Huffman, J. C.; Lewis, L. N.; Caulton, K. G. *Inorg. Chem.* **1980**, *19*, 2755.

Table II. Fractional Coordinates and Isotropic Thermal Parameters for $[Ir(C_2H_4)_2(PMe_2Ph)_3]BF_4 \cdot 0.5H_2O$

	10^4x	10^4y	10^4z	$10B_{iso}$
Ir(1A)	5278 (1)	2435.6 (3)	270.9 (2)	13
C(2A)	5137 (17)	3093 (9)	867 (6)	25
C(3A)	5523 (17)	3457 (8)	475 (6)	21
C(4A)	5535 (17)	2463 (8)	9502 (6)	21
C(5A)	5458 (15)	1796 (8)	9656 (6)	16
P(6A)	4878 (5)	1516 (2)	754 (2)	20
C(7A)	5936 (16)	1386 (12)	1295 (7)	35
C(8A)	5003 (20)	736 (9)	455 (8)	35
C(9A)	3328 (19)	1481 (9)	1017 (7)	27
C(10A)	2350 (18)	1072 (9)	813 (7)	30
C(11A)	1222 (16)	1094 (9)	1012 (7)	29
C(12A)	970 (19)	1473 (12)	1410 (7)	38
C(13A)	1919 (19)	1884 (10)	1599 (7)	33
C(14A)	3106 (18)	1882 (9)	1420 (6)	25
P(15A)	3148 (4)	2671 (2)	21 (1)	14
C(16A)	1998 (15)	2812 (8)	464 (5)	15
C(17A)	2336 (17)	2072 (8)	−365 (6)	21
C(18A)	2929 (15)	3430 (9)	9679 (5)	17
C(19A)	2766 (18)	4038 (9)	9903 (6)	25
C(20A)	2626 (18)	4632 (8)	9654 (7)	27
C(21A)	2531 (18)	4615 (11)	9151 (9)	39
C(22A)	2661 (16)	4005 (12)	−1093 (7)	34
C(23A)	2843 (17)	3428 (9)	−834 (6)	23
P(24A)	7486 (4)	2362 (2)	425 (2)	16
C(25A)	8105 (17)	2596 (10)	1017 (6)	26
C(26A)	8259 (19)	1574 (10)	351 (7)	30
C(27A)	8372 (17)	2880 (9)	33 (6)	25
C(28A)	8722 (17)	3513 (9)	160 (8)	31
C(29A)	9388 (19)	3917 (12)	9863 (10)	47
C(30A)	9674 (19)	3678 (13)	9435 (9)	49
C(31A)	9355 (22)	3032 (12)	−720 (9)	48
C(32A)	8725 (15)	2638 (11)	9583 (6)	27
Ir(1B)	6653 (1)	600.5 (3)	7481.3 (2)	12
C(2B)	6635 (16)	−352 (8)	7818 (6)	16
C(3B)	6953 (16)	9553 (8)	7337 (6)	19
C(4B)	6817 (16)	981 (8)	6759 (6)	18
C(5B)	6758 (14)	1511 (7)	7095 (6)	13
P(6B)	6159 (4)	1141 (2)	8196 (2)	18
C(7B)	5715 (16)	583 (8)	8673 (6)	19
C(8B)	7299 (18)	1637 (9)	8538 (6)	26
C(9B)	4866 (17)	1723 (8)	8141 (6)	20
C(10B)	5019 (19)	2320 (9)	7884 (6)	27
C(11B)	4054 (22)	2769 (9)	7802 (7)	33
C(12B)	2890 (22)	2655 (10)	7969 (7)	37
C(13B)	2669 (19)	2114 (11)	8235 (7)	35
C(14B)	3676 (19)	1658 (10)	8328 (6)	29
P(15B)	8873 (4)	658 (2)	7625 (1)	16
C(16B)	9604 (17)	41 (9)	8032 (7)	24
C(17B)	9622 (17)	1387 (9)	7881 (6)	26
C(18B)	9738 (15)	560 (9)	7067 (6)	20
C(19B)	173 (17)	9960 (8)	6938 (6)	21
C(20B)	10761 (18)	−125 (11)	6509 (7)	33
C(21B)	10883 (18)	394 (14)	6212 (7)	51
C(22B)	10503 (17)	1012 (13)	6346 (6)	39
C(23B)	9908 (16)	1097 (9)	6780 (6)	21
P(24B)	4500 (4)	457 (2)	7224 (1)	14
C(25B)	3401 (18)	123 (8)	7640 (6)	22
C(26B)	3634 (17)	1190 (9)	7027 (6)	22
C(27B)	4184 (16)	9906 (8)	6707 (6)	18
C(28B)	3939 (17)	−760 (9)	6769 (6)	22
C(29B)	3699 (17)	8824 (9)	6381 (7)	24
C(30B)	3788 (17)	9070 (10)	5915 (6)	26
C(31B)	4037 (18)	9707 (9)	5845 (6)	24
C(32B)	4236 (16)	116 (8)	6230 (7)	21
B(1)	8753 (26)	1797 (11)	2483 (8)	35
F(2)	9086 (14)	2267 (6)	2148 (4)	50
F(3)	8324 (15)	1242 (7)	2279 (6)	70
F(4)	8098 (19)	2077 (7)	2818 (6)	86
F(5)	9927 (17)	1596 (6)	2724 (7)	98
B(6)	8104 (26)	9668 (12)	769 (10)	39
F(7)	8952 (15)	9186 (7)	959 (5)	66
F(8)	8463 (23)	9817 (11)	314 (7)	123
F(9)	8130 (18)	10216 (7)	1036 (6)	83
F(10)	6923 (13)	9404 (7)	682 (6)	66
O(11)	8601 (21)	4436 (12)	4436 (8)	116 (6)

Table III. Selected Bond Distances (Å) and Angles (deg) for $[Ir(C_2H_4)_2(PMe_2Ph)_3]BF_4 \cdot 0.5H_2O$

Ir(1A)–P(6A)	2.356 (5)	Ir(1B)–P(6B)	2.357 (4)
Ir(1A)–P(15A)	2.363 (5)	Ir(1B)–P(15B)	2.359 (5)
Ir(1A)–P(24A)	2.351 (5)	Ir(1B)–P(24B)	2.360 (5)
Ir(1A)–C(2A)	2.140 (16)	Ir(1B)–C(2B)	2.151 (16)
Ir(1A)–C(3A)	2.164 (16)	Ir(1B)–C(3B)	2.194 (16)
Ir(1A)–C(4A)	2.171 (15)	Ir(1B)–C(4B)	2.169 (16)
Ir(1A)–C(5A)	2.166 (16)	Ir(1B)–C(5B)	2.145 (15)
C(2A)–C(3A)	1.401 (25)	C(2B)–C(3B)	1.411 (22)
C(4A)–C(5A)	1.427 (24)	C(4B)–C(5B)	1.431 (23)
P(6A)–Ir(1A)–P(15A)	97.11 (16)	P(6B)–Ir(1B)–P(15B)	96.23 (1)
P(6A)–Ir(1A)–P(24A)	93.47 (16)	P(6B)–Ir(1B)–P(24B)	92.80 (1)
P(6A)–Ir(1A)–C(2A)	91.8 (5)	P(6B)–Ir(1B)–C(2B)	92.6 (4)
P(6A)–Ir(1A)–C(3A)	129.5 (5)	P(6B)–Ir(1B)–C(3B)	130.5 (5)
P(6A)–Ir(1A)–C(4A)	128.3 (5)	P(6B)–Ir(1B)–C(4B)	130.5 (5)
P(6A)–Ir(1A)–C(5A)	90.1 (4)	P(6B)–Ir(1B)–C(5B)	92.3 (4)
P(15A)–Ir(1A)–P(24A)	169.41 (15)	P(15B)–Ir(1B)–P(24B)	170.97 (15)
P(15A)–Ir(1A)–C(2A)	89.2 (5)	P(15B)–Ir(1B)–C(2B)	90.5 (5)
P(15A)–Ir(1A)–C(3A)	88.7 (5)	P(15B)–Ir(1B)–C(3B)	85.7 (5)
P(15A)–Ir(1A)–C(4A)	83.4 (5)	P(15B)–Ir(1B)–C(4B)	89.9 (5)
P(15A)–Ir(1A)–C(5A)	91.3 (4)	P(15B)–Ir(1B)–C(5B)	87.6 (4)
P(24A)–Ir(1A)–C(2A)	91.1 (5)	P(24B)–Ir(1B)–C(2B)	89.1 (5)
P(24A)–Ir(1A)–C(3A)	85.0 (5)	P(24B)–Ir(1B)–C(3B)	88.5 (5)
P(24A)–Ir(1A)–C(4A)	89.6 (5)	P(24B)–Ir(1B)–C(4B)	84.2 (5)
P(24A)–Ir(1A)–C(5A)	88.1 (4)	P(24B)–Ir(1B)–C(5B)	92.1 (4)
C(2A)–Ir(1A)–C(3A)	38.0 (7)	C(2B)–Ir(1B)–C(3B)	37.9 (6)
C(2A)–Ir(1A)–C(4A)	139.8 (7)	C(2B)–Ir(1B)–C(4B)	136.6 (6)
C(2A)–Ir(1A)–C(5A)	178.0 (7)	C(2B)–Ir(1B)–C(5B)	174.6 (6)
C(3A)–Ir(1A)–C(4A)	102.2 (6)	C(3B)–Ir(1B)–C(4B)	99.0 (6)
C(3A)–Ir(1A)–C(5A)	140.1 (6)	C(3B)–Ir(1B)–C(5B)	137.2 (6)
C(4A)–Ir(1A)–C(5A)	38.4 (6)	C(4B)–Ir(1B)–C(5B)	38.7 (6)

Table IV. Crystal Data for $[Ir(C_3H_4)_2(PMe_2Ph)_3]BF_4$

empirical formula	$IrP_3F_4C_{30}BH_{41}$
color	colorless
crystal dimensions	0.1 × 0.3 × 0.4 mm
space group	$P2_1/a$
cell dimensions (at −158 °C)	
a =	21.817 (7) Å
b =	13.999 (2) Å
c =	10.022 (1) Å
β =	92.91 (1)°
molecules/cell	4
volume (Å^3)	3057.01
calcd density (gm/cm^3)	1.681
wavelength (Å)	0.71069
molecular weight	773.60
linear absorption coeff (cm^{-1})	45.5
no. of unique intensities	4005
no. with $F > 0.0$	3796
no. with $F > 2.33\sigma(F)$	3548
final residuals	
$R(F)$	0.0537
$R_w(F)$	0.0542
goodness of fit for last cycle	1.50
max Δ/σ for last cycle	0.027

Crystallography of $[Ir(C_3H_4)_2(PMe_2Ph)_3]BF_4$. An irregular wedge-shaped crystal, grown by layering a CH_2Cl_2 solution with Et_2O, proved to be single and was mounted by using silicone grease and transferred to a goniostat where it was cooled to −158 °C for characterization and data collection. A systematic search of a limited hemisphere of reciprocal space revealed Laue symmetry and systematic absences consistent with space group $P2_1/a$. Data processing gave a residual of 0.04 for 359 unique intensities which had been measured more than once. Four standards measured every 300 data showed no systematic trends, and no absorption correction was applied. Characteristics of the data collection[5] ($6° \le 2\theta \le 45°$), processing, and refinement are given in Table IV.

The structure was solved by using a combination of direct methods (MULTAN78) and Fourier techniques. All hydrogens were placed in fixed calculated positions, and all non-hydrogen atoms were refined anisotropically. The final least-squares had an $R(F) = 0.054$. The final difference map had several peaks between 1 and 2 e/Å^3. Most of them were Ir residuals; one was near C(30) in one of the allene groups, and two of them were near C(4), one of the methyl groups. All other residual peaks were less than 1 e/Å^3. The results of the X-ray study are given in Tables V and VI and Figure 2. The BF_4^- ion is unexceptional, BF distances ranging from 1.33 (2) to 1.39 (2) Å with FBF angles between 106.4 (14) and 112.2 (16)°.

Table V. Fractional Coordinates[a] and Isotropic Thermal Parameters[b] for $[Ir(C_3H_4)_2(PMe_2Ph)_3]BF_4$

atom	x	y	z	$10B_{iso}$
Ir(1)	3817.3 (2)	8195.6 (3)	1341.6 (4)	13
P(2)	4225 (1)	6635 (2)	1060 (3)	15
C(3)	4119 (6)	5709 (8)	2302 (12)	21
C(4)	3907 (5)	6031 (9)	−408 (12)	20
C(5)	5048 (5)	6618 (8)	869 (12)	16
C(6)	5459 (6)	6623 (8)	1981 (12)	20
C(7)	6076 (5)	6681 (9)	1829 (15)	25
C(8)	6311 (6)	6744 (9)	587 (14)	26
C(9)	5925 (6)	6707 (9)	9474 (12)	22
C(10)	5293 (6)	6664 (8)	9576 (13)	22
P(11)	4107 (1)	8394 (2)	3665 (3)	19
C(12)	4851 (7)	8937 (10)	3932 (14)	33
C(13)	3627 (6)	9133 (10)	4667 (12)	27
C(14)	4154 (6)	7324 (9)	4716 (11)	20
C(15)	3610 (6)	6855 (10)	5007 (12)	23
C(16)	3641 (8)	6033 (12)	5751 (14)	39
C(17)	4191 (9)	5662 (11)	6167 (14)	42
C(18)	4731 (7)	6116 (11)	5923 (12)	32
C(19)	4706 (6)	6951 (9)	5198 (12)	25
P(20)	3369 (1)	9733 (2)	1150 (3)	16
C(21)	2634 (6)	9885 (9)	1922 (13)	24
C(22)	3835 (6)	10741 (9)	1813 (13)	23
C(23)	3192 (5)	99 (8)	9401 (11)	16
C(24)	2666 (5)	9759 (8)	−1298 (11)	17
C(25)	2546 (6)	10000 (9)	−2613 (15)	28
C(26)	2924 (6)	623 (8)	6768 (12)	21
C(27)	3433 (7)	978 (10)	7458 (13)	29
C(28)	3573 (5)	10732 (9)	−1255 (12)	20
C(29)	4670 (5)	8815 (9)	694 (11)	18
C(30)	4284 (5)	8478 (8)	−390 (12)	19
C(31)	4218 (6)	8396 (10)	−1700 (13)	27
C(32)	2947 (5)	7558 (9)	1862 (12)	20
C(33)	2992 (5)	7663 (9)	474 (12)	17
C(34)	2727 (6)	7493 (10)	−679 (14)	26
B(35)	3284 (8)	2692 (15)	4340 (18)	37
F(36)	2948 (4)	3125 (8)	5310 (8)	51
F(37)	3799 (4)	2281 (8)	4932 (9)	51
F(38)	3424 (6)	3298 (10)	3377 (12)	90
F(39)	2924 (5)	1964 (10)	3810 (12)	78

[a] Fractional coordinates are ×10⁴. [b] Isotropic values for those atoms refined anisotropically are calculated by using the formula given by Hamilton, W. C. *Acta Crystallogr.* **1959**, *12*, 609.

Table VI. Selected Bond Distances (Å) and Angles (deg) for $[Ir(C_3H_4)_2(PMe_2Ph)_3]BF_4$

Ir(1)–P(2)	2.381 (3)	Ir(1)–C(33)	2.097 (11)
Ir(1)–P(11)	2.398 (3)	C(29)–C(30)	1.421 (17)
Ir(1)–P(20)	2.368 (3)	C(30)–C(31)	1.318 (18)
Ir(1)–C(29)	2.181 (11)	C(32)–C(33)	1.408 (17)
Ir(1)–C(30)	2.094 (12)	C(33)–C(34)	1.288 (17)
Ir(1)–C(32)	2.185 (11)		
P(2)–Ir(1)–P(11)	98.03 (10)	C(29)–Ir(1)–C(32)	176.5 (4)
P(2)–Ir(1)–P(20)	168.43 (10)	C(29)–Ir(1)–C(33)	138.2 (4)
P(2)–Ir(1)–C(29)	90.0 (3)	C(30)–Ir(1)–C(32)	137.8 (5)
P(2)–Ir(1)–C(30)	82.8 (3)	C(30)–Ir(1)–C(33)	99.6 (5)
P(2)–Ir(1)–C(32)	89.3 (3)	C(32)–Ir(1)–C(33)	38.3 (4)
P(2)–Ir(1)–C(33)	86.7 (3)	C(24)–C(25)–C(26)	120.1 (12)
P(11)–Ir(1)–P(20)	93.49 (11)	C(25)–C(26)–C(27)	119.6 (12)
P(11)–Ir(1)–C(29)	93.2 (3)	C(26)–C(27)–C(28)	121.7 (13)
P(11)–Ir(1)–C(30)	131.9 (3)	C(23)–C(28)–C(27)	119.9 (12)
P(11)–Ir(1)–C(32)	90.3 (3)	Ir(1)–C(29)–C(30)	67.3 (7)
P(11)–Ir(1)–C(33)	128.5 (3)	Ir(1)–C(30)–C(29)	73.9 (7)
P(20)–Ir(1)–C(29)	88.2 (3)	Ir(1)–C(30)–C(31)	140.8 (10)
P(20)–Ir(1)–C(30)	88.7 (3)	Ir(1)–C(32)–C(33)	67.5 (6)
P(20)–Ir(1)–C(32)	91.7 (3)	Ir(1)–C(33)–C(32)	74.2 (7)
P(20)–Ir(1)–C(33)	87.0 (3)	Ir(1)–C(33)–C(34)	140.8 (10)
C(29)–Ir(1)–C(30)	38.8 (5)		

Results

Characterization of $IrH_4P_3^+$. When IrH_3P_3 (P = PMe_2Ph) is protonated with the strong acid $HBF_4{\cdot}OEt_2$ in CH_2Cl_2, the complex $IrH_4P_3^+$ is formed.[3] We showed earlier that the A_4X_3 spin system, indicative of fluxionality, could be frozen out to an X_2Y $^{31}P\{^1H\}$ pattern at −80 °C but could not be slowed at −80 °C in the 360 MHz ^1H NMR. T_1 measurements at −70 °C in CD_2Cl_2 reveal a spin–lattice relaxation time of 20 ms for the time-averaged resonance of all four H ligands. Comparison of this T_1 value with the values (Table VII) of other dihydrogen and hydride complexes[6] clearly support the interpretation that this cation contains a coordinated dihydrogen molecule. We suggest the formulation $Ir(H)_2(\eta^2\text{-}H_2)P_3^+$, which gives the very common six-coordinate octahedral geometry favored by Ir(III). This structure is also supported by earlier chemical reactivity studies of $IrH_4P_3^+$, **1** which

Table VII. T_1 Values for some Hydrides[6]

complex	T_1[a] (ms)	type of structure
$RuH_4(PPh_3)_3$	38	dihydrogen
$FeH_4(PEtPh_2)_3$	24	dihydrogen
$OsH_4(P(p\text{-tolyl}))_3$	820	hydride
$IrH_3(PMe_2Ph)_3$	465[b]	hydride
$IrH_4(PMe_2Ph)_3^+$	20[b]	dihydrogen
$IrH_5(PCy_3)_2$	820	hydride

[a] T_1 values at ~200 K in CD_2Cl_2 or toluene-d_8. [b] This work.

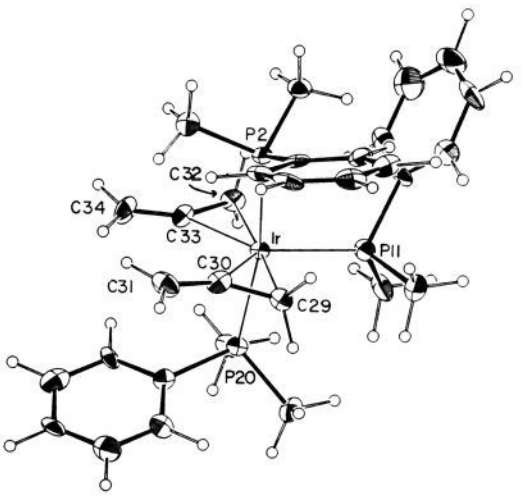

Figure 2. ORTEP drawing of $Ir(C_3H_4)_2(PMe_2Ph)_3^+$.

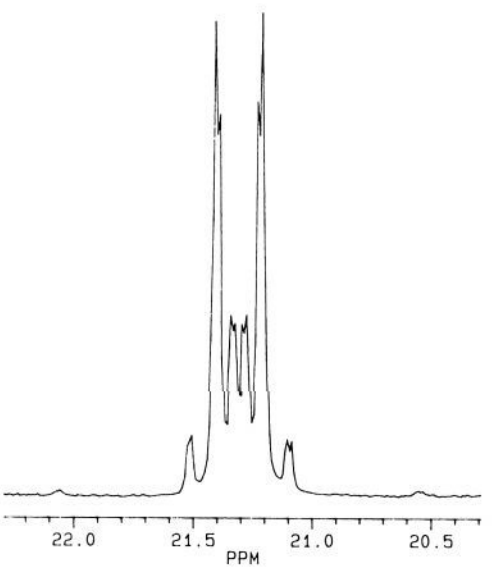

Figure 3. $^{13}C\{^1H\}$ NMR of the ethylene carbons in $Ir(^{13}C_2H_4)(CH_3CN)(PMe_2Ph)_3^+$ showing the magnetically inequivalent carbons (AA′XX′).

(6) Crabtree, R. H.; Hamilton, D. G. *J. Am. Chem. Soc.* **1988**, *110*, 4126.

suggest the occurrence of eq 1. For example, we reported earlier that the 16-electron equilibrium participant $IrH_2P_3^+$ can be captured by CO, MeCN, THF, and D_2.[3]

$$\underset{\mathbf{1}}{IrH_4P_3^+} \rightleftharpoons IrH_2P_3^+ + H_2 \qquad (1)$$

Reaction of $IrH_4P_3^+$ with Ethylene. The ready reversible dissociation of H_2 from $IrH_4P_3^+$ furnishes a rare 16-electron hydride species which can also be trapped by the reducible substrate C_2H_4. Addition of excess ethylene to **1** in CH_2Cl_2 gives a 97% yield of a cream-colored powder **2**. The ^1H NMR of this material shows no remaining hydride ligands but does show resonances for two coordinated ethylene molecules. The $^{13}C\{^1H\}$ NMR spectrum of **2** shows two ethylene carbon environments at and above room temperature and, together with the $^{31}P\{^1H\}$ NMR spectrum, suggests a rare,[7,8] stereochemically rigid, five-coordinate iridium cation with equivalent nonrotating (−80 to +80 °C) ethylene ligands: $Ir(C_2H_4)_2P_3^+$. The C/C coupling constant within coordinated ethylene (44 Hz) is substantially reduced from the value[9] in free ethylene (67 Hz). The solid-state structure determination (Figure 1) is consistent with the spectral parameters and reveals a trigonal-bipyramidal arrangement around iridium with two ethylenes and one phosphine unit occupying the equatorial sites. This planar equatorial positioning of the ethylene ligands is as predicted for a d^8 TBP arrangement.[10] Distortions from perfect trigonal-bipyramidal geometry are evident (Table III). The axial phosphines deviate from linearity (170°), bending away from the equatorial phosphine. Within the equatorial plane, the angle between the two ethylene midpoints is larger than 120° (137° and 140°).

When the reaction of $Ir(H)_2(H_2)P_3^+$ with excess ethylene is monitored by ^1H NMR at −50 °C, an ethylene adduct of the H_2-loss product $IrH_2P_3^+$, *cis,mer*-$IrH_2(C_2H_4)P_3^+$ (**3**), can be observed. Over time, the resonances for **3** subsequently decrease, while those of the bis-olefin complex **2** and of ethane appear. However, in the absence of excess ethylene, even at room temperature, the hydrido–olefin complex **3** is stable and does not eliminate ethane. Thus, *the reduction of ethylene to ethane is ethylene-promoted*. Compound **3** can also be generated by the reaction of **2** with H_2 (eq 2). The curious elimination of *ethylene*

$$\underset{\mathbf{2}}{P_3Ir(C_2H_4)_2^+} + H_2 \rightarrow \underset{\mathbf{3}}{\textit{cis,mer}\text{-}IrH_2(C_2H_4)P_3^+} + C_2H_4 \qquad (2)$$

(not ethane) in this reaction is explained by an independent examination of the reactivity of **2**. We find that the characteristic reaction of **2** is reversible ethylene dissociation (eq 3). This is

$$\underset{\mathbf{2}}{Ir(C_2H_4)_2P_3^+} \rightleftharpoons Ir(C_2H_4)P_3^+ + C_2H_4 \qquad (3)$$

most directly demonstrated by the observation that **2** exchanges within 30 min with ^{13}C-labeled ethylene. Thus, ethylene is a product of eq 2 because this reaction is initiated by C_2H_4 loss from **2**, followed by trapping of $Ir(C_2H_4)P_3^+$ by H_2.

The equilibrium species $Ir(C_2H_4)P_3^+$ of eq 3 can also be trapped with CH_3CN. The spectral data for $Ir(C_2H_4)(NCMe)P_3^+$ uniquely define its structure as **4a** (L = MeCN) below. In particular,

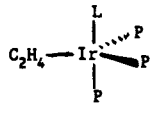

4a

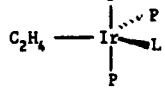

4b

the observation of two ethylene hydrogen types but a single ethylene carbon chemical shift excludes **4b** and supports **4a**. The AA′XX′ spin system in the $^{13}C\{^1H\}$ NMR spectrum of the compound from 99% ^{13}C-labeled ethylene (Figure 3) is also consistent with **4a**.[11] Stereochemistry **4a** is also indicated by the AX_2 $^{31}P\{^1H\}$ pattern, the PMe ^1H NMR pattern (a doublet and two virtual triplets), and the AA′BXX′ pattern in the $^{31}P\{^1H\}$ spectrum of the product from 99% $^{13}C_2H_4$. These observations are, of course, remarkable in that they indicate the absence of rapid olefin rotation and also the stereochemical rigidity of the trigonal-bipyramidal coordination geometry.

Similarly, MeLi can be used to trap $Ir(C_2H_4)P_3^+$ in eq 3, forming the neutral, nonfluxional methyl–ethylene complex, $IrMe(C_2H_4)P_3$ (**4a**, L = CH_3^-). The stereochemistry **4a** is based on ^{13}C, ^{31}P, and ^1H NMR results (see Experimental Section).

Addition of D_2 to the bis-ethylene complex **2** initially generates the isotopomer $IrD_2(C_2H_4)P_3^+$, which shows rapid incorporation of deuterium into the ethylene and points to the reversibility of eq 4. Equation 4, alone, is not sufficient to explain the observed

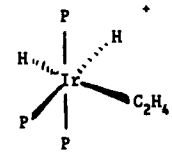

$$\underset{\mathbf{3}}{} \quad = \quad \underset{\mathbf{A}}{Ir(CH_2CH_3)HP_3^+} \qquad (4)$$

scrambling of *both* cis and trans hydride positions of **3** with all ethylene hydrogens of $IrD_2(C_2H_4)P_3^+$, since the hydrides in **3** are chemically inequivalent. However, since **3** exchanges with (1 atm) D_2 at a rate comparable to that of eq 4, an equilibrium H_2-elimination from **3** must also occur (eq 5). Note that this equilibrium involves the same 16-electron species implicated in eq 3. An alternative mechanism for incorporation of D_2 into **3** involves addition of D_2 to $IrEt(H)P_3^+$, H/D site exchange, elimination of HD, and then β-hydrogen elimination (eq 4) producing **3**-d_1.

$$\underset{\mathbf{3}}{H_2Ir(C_2H_4)P_3^+} \rightleftharpoons H_2 + Ir(C_2H_4)P_3^+ \qquad (5)$$

Neither $IrEt(H)P_3^+$ nor the expected hydrido/ethyl/ethylene species ($HIr(C_2H_5)(C_2H_4)P_3^+$) "downstream" of eq 4 has been observed under a variety of conditions. However, when methyl acrylate is substituted for ethylene, the hydrido alkyl complex **5**

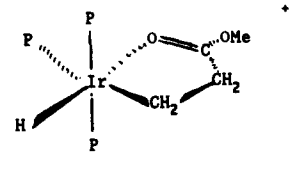

5

can be isolated in near quantitative yield. The spectral assignment of this rare,[12] octahedral cis hydrido–alkyl complex deserves some comment. The $^{31}P\{^1H\}$ NMR reveals an AB_2 pattern, consistent with a meridonal phosphine unit. In the ^1H NMR, a single hydride resonance is observed which shows small H–P couplings corresponding to only cis hydride–phosphine relationships. The upfield shift for the hydride signal (−27.75 ppm) is characteristic of a hydride trans to a weakly donating ligand. For example, in the related complexes, *cis,mer*-$IrH_2(THF)P_3^+$[3] and *cis,mer*-$IrH_2(Me_2CO)P_3^+$,[13] the hydride trans to the solvent molecule shows a resonance upfield at −24.5 and −28.3 ppm, respectively. The infrared spectrum also supports this arrangement with an Ir–H frequency (2240 cm^{-1}) diagnostic of a hydride trans to a weak donor ligand[14,15] and a carbonyl band (1750 cm^{-1}) consistent with an ester retaining a strong C/O bond.

(7) Shapley, J. R.; Osborn, J. A. *Acc. Chem. Res.* **1973**, *6*, 305.
(8) Another stereochemically rigid, five-coordinate complex with nonrotating ethylene ligands is $Os(PMe_3)_2(C_2H_4)_2(CO)$. See: Kiel, G.-Y.; Takats, J.; Grevels, F. W. *J. Am. Chem. Soc.* **1987**, *109*, 2227.
(9) Gunter, H. *Angew. Chem., Int. Ed. Engl.* **1972**, *11*, 861.
(10) Rossi, A. R.; Hoffmann, R. *Inorg. Chem.* **1975**, *14*, 365.
(11) C–P_{axial} coupling is negligible, as is confirmed by the simple triplet for the $^{31}P\{^1H\}$ spectrum of the axial P in $Ir(^{13}C_2H_4)(MeCN)P_3^+$. Note that C–$P_{axial}$ coupling is also unobserved in $Ir(^{13}C_2H_4)_2(PMe_2Ph)_3^+$.
(12) Halpern, J. *Inorg. Chim. Acta* **1981**, *50*, 11.
(13) Westerberg, D. E. (Indiana University). Unpublished results.
(14) Appleton, T. G.; Clark, H. C.; Manzer, L. E. *Coord. Chem. Rev.* **1973**, *10*, 335.
(15) Crabtree, R. H.; Demou, P. C.; Eden, D.; Mihelcic, J. M.; Parnell, C. A.; Quirk, J. M.; Morris, G. E. *J. Am. Chem. Soc.* **1982**, *104*, 6994.

Scheme I

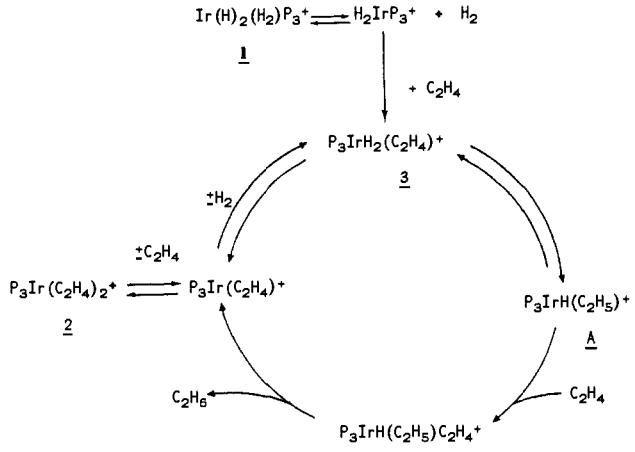

Incorporation of all the above experimental evidence leads to the following cycle for the hydrogenation of ethylene by $Ir(H)_2(H_2)P_3^+$ (Scheme I). In this scheme, numbered compounds have been detected and/or isolated. Compound A is inferred from the reactivity studies. Reactions shown as equilibria have been directly demonstrated to be reversible.

Reaction of $IrH_4P_3^+$ with Allene. We were interested in examining the generality of the reactivity of $IrH_4P_3^+$ with olefins. Addition of excess allene to a CH_2Cl_2 solution of $IrH_4P_3^+$, followed by stirring for 10 h, leads to the formation of a colorless material in high yield. The $^{31}P\{^1H\}$ NMR reveals an AB_2 pattern, while the ^1H NMR shows the absence of hydride ligands and the presence of complex resonances centered at 1.65, 5.50, and 6.30 ppm. Integration of these resonances versus the PMe_2Ph intensity signals a stoichiometry consistent with $Ir(C_3H_4)_2P_3^+$. The $^{13}C\{^1H\}$ NMR shows only three resonances for the allene ligands consistent with a product containing two symmetry-equivalent C_3 fragments. Unfortunately, these spectral data do not distinguish between a bis-allene complex **6a** and a product in which the two allene ligands are coupled, **6a**.[16] Both **6a** and **6b** would show three separate

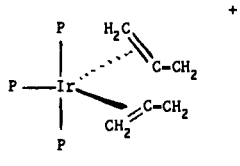

6a

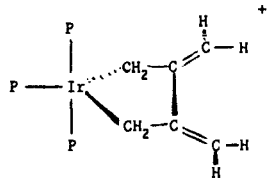

6b

signals in both the ^1H and ^{13}C NMR for the C_3H_4-derived ligands. Since the exact nature of this product could not be unambiguously determined by spectroscopic methods, a solid-state structure determination was carried out.

The X-ray structure reveals (Figure 2) that $Ir(C_3H_4)_2P_3^+$ (**6a**) contains two uncoupled allene ligands. This trigonal-bipyramidal cation resembles $Ir(C_2H_4)_2P_3^+$ with the two allenes and one phosphine ligand occupying the equatorial positions. The allene ligands in **6a** are bent (145°) in a fashion found in all η^2-allene complexes.[17,18] Coordination of allene also lengthens the coordinated C=C bond by 0.1 Å compared to that of the noncoordinated allene double bond. In an effort to minimize steric interactions, the axial phosphines bend away from the equatorial phosphine just as they do in $Ir(C_2H_4)_2P_3^+$.

When the reaction of $IrH_4P_3^+$ with excess allene is monitored at −60 °C by ^1H NMR in CD_2Cl_2, no hydride-containing intermediates are observed. The ^1H NMR reveals the production of propene together with resonances for a bis-allene complex "X" different from **6a**. Complex "X" can be isolated, redissolved in CD_2Cl_2 at 20 °C, and shown to convert over a period of 6 h

Chart I

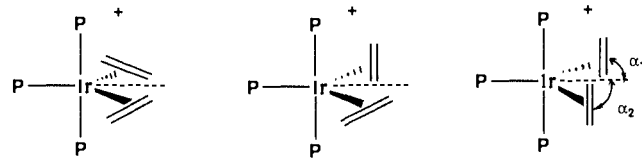

exclusively to complex **6a**. This demonstrates that conversion of "X" to **6a** takes place even in the absence of excess allene, and thus the intermediate must contain two allene ligands. Conversion of "X" is thus an isomerization. ^1H NMR indicates that the allene ligands in "X" are not related by symmetry; six resonances are observed for the eight allene protons. This inequivalence is also indicated by the presence of distereotopic methyl groups on the mutually trans phosphine ligands. The $^{13}C\{^1H\}$ NMR spectrum shows six resonances for the two inequivalent allene ligands. These spectral data are consistent with the following unsymmetrical structure for this initial, bis-allene product **6c**.

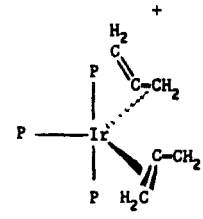

6c

The thermodynamic product **6a** reacts slowly ($t_{1/2}$ = 10 days) with H_2 (1 atm) in CD_2Cl_2 to liberate propane and produce $IrH_4P_3^+$, without the observation of a hydrido olefin intermediate. This result, along with the inability of CH_3CN to displace allene (or trap a monoallene cation), demonstrates the small equilibrium constant associated with the following equilibrium (eq 6). Such behavior is in contrast to that of the bis-ethylene complex **2**, which readily loses ethylene (eq 3).

$$\underset{\mathbf{6a}}{Ir(C_3H_4)_2P_3^+} \rightleftharpoons Ir(C_3H_4)P_3^+ + C_3H_4 \qquad (6)$$

The Origin of the Observed Molecular Structure and Dynamics. The above observations necessitate answers to the following questions: (1) Why are trigonal-bipyramidal $Ir(olefin)_2(PMe_2Ph)_3^+$ (olefin = ethylene or allene) stereochemically rigid with regard to axial/equatorial site exchange via, for example, Berry pseudorotation? (2) Why is there a large barrier for rotation of either ethylene or allene out of the equatorial plane? This question is associated with understanding why the ground state has the olefin axis perpendicular to the pseudo-3-fold axis of the trigonal bipyramid.

This study will be divided in two parts: one concerning the rotation of the olefins and the other concerning some aspects of the pseudorotation at the metal. The rotation of an olefin in a trigonal bipyramid is the superposition of essentially two motions: the rigid[19] rotation of the olefin and the transformation of the TPB into a square pyramid (a step on the way to the Berry pseudorotation). This change of coordination geometry has been shown to ease considerably the rigid rotation barrier.[20] Due to the complexity of the present problem (arising from its total lack of symmetry), we have chosen to dissociate the two motions and to study them separately. We will compare the rigid rotation of the present bis-olefin to several monoolefin complexes where more experimental data are known. It can be reasonably assumed that the TBP/square pyramid transformation will not reverse the order found for the rigid rotation.

(16) Structure **6b** could achieve an 18-electron count by coordinating BF_4^-.
(17) Shaw, B. L.; Stringer, A. J. *Inorg. Chim. Acta Rev.* **1973**, *7*, 1.
(18) Otsuka, S.; Nakamura, A. *Adv. Organomet. Chem.* **1976**, *14*, 245.

(19) By this term, we mean rotation with the IrP_3(olefin) geometry maintained as a fragment of a trigonal bipyramid.
(20) Albright T. A.; Hoffmann, R.; Thibeault, J. C.; Thorn, D. L. *J. Am. Chem. Soc.* **1979**, *101*, 3801.

Table VIII. Atomic Parameters[d]

atom	orbital	ζ	H_{ii} (eV)
Ir[a]	6s	2.50	−11.36
	6p	2.20	−4.50
	5d	5.796 (0.63506)	−12.17
		2.557 (0.55560)	
P[b]	3s	1.60	−18.60
	3p	1.60	−14.0
C[c]	2s	1.625	−21.4
	2p	1.625	−11.4
O[c]	2s	2.275	−32.3
	2p	2.275	−14.8
H[c]	1s	1.3	−13.6

[a] Dubois, D. L.; Hoffmann, R. *Nouv. J. Chim.* **1977**, *1*, 479. [b] Summerville, R. H.; Hoffmann, R. *J. Am. Chem. Soc.* **1976**, *98*, 7240. [c] Hoffmann, R. *J. Chem. Phys.* **1963**, *39*, 1397. [d] Numbers in parentheses correspond to the coefficients of a double-ζ expansion of the d orbital.

(1) Rigid Rotation of the Olefin. The model compound chosen for the calculations is $Ir(C_2H_4)_2(PH_3)_3^+$, with use of bond lengths taken from the experimental structure. The calculations were done with the EHT method with weighted H_{ij}.[21] The parameters given in Table VIII were chosen from previous references.

The structures of three conformers are shown in Chart I. Keeping a trigonal ligand field at the metal (P–Ir–P angles of 180° and 90°), the optimal angle between the two Iridium–ethylene midpoints is calculated to be 132°, which is in excellent agreement with the experimental value. Rotation of one olefin by 90° costs 50 kcal/mol. The rotation of the olefin requires some displacement of the olefin midpoints in the equatorial plane. The olefin midpoint of the rotated olefin is moved toward the equatorial phosphine, $\alpha_1 = 86°$, while the midpoint of the other olefin is moved away from the equatorial phosphine, $\alpha_2 = 45°$. Finally, rotating the other olefin costs an additional 71 kcal/mol, the angle between the olefin midpoints now being 122°.

It is clear that the rigid rotation of an olefin, not to mention that of two olefins, is a disfavored process. In order to understand the reasons for the high energy of this process, we have undertaken similar calculations on a monoolefinic complex, to assign the role of the second olefin in the activation energy.

The preferred conformation of the hypothetical $Ir(C_2H_4)(PH_3)_4^+$ corresponds to the ethylene in the equatorial plane. Rotating the ethylene by 90° costs 47 kcal/mol. In contrast, replacement of all the phosphines in this molecule by CO ligands considerably lowers the rotation barrier to 21 kcal/mol, a value comparable to that calculated by Hoffmann and co-workers for the $Fe(C_2H_4)(CO)_4$ complex.[20]

It is thus apparent that the presence of accompanying π-acceptor ligands considerably lowers the rotation barrier. In order to assess the relative importance of the apical and the equatorial CO ligands in this effect, we have calculated the olefin rotation barrier in another model complex, $Ir(C_2H_4)(PH_3)_2(CO)_2^+$. When both phosphine ligands are in the equatorial plane, the rotation barrier is calculated to be 24 kcal/mol, i.e., close to the tetracarbonyl case. In contrast, if the phosphine ligands are apical, the rotation barrier is calculated to be 43 kcal/mol, i.e., closer to the rotation barrier calculated for $Ir(C_2H_4)(PH_3)_4^+$. *The high rotation barrier is thus due to the absence of π-acceptor ligands at the apical site.* The absence of apical π-acceptor ligands in $Ir(C_2H_4)(MeCN)P_3^+$ and $IrMe(C_2H_4)P_3$ is likewise the reason for the experimentally observed rigidity of both complexes.

An analysis of the interaction of the L_4Ir^+ fragment orbitals with ethylene orbitals reveals the reasons for this behavior. The rotation of an olefin in a trigonal bipyramid has been studied in detail by various authors,[22a] and we will extract the arguments germane to our analysis. The conformational preference of an olefin is associated to the interaction of olefin π^*_{CC} with an occupied metal orbital of appropriate symmetry. When the olefin lies in the equatorial plane, π^*_{CC} interacts with the HOMO (mainly *xy*) of L_4Ir^+, **7**. The overlap (0.24) between the metal HOMO and π^*_{CC} is large since the orbital is strongly hybridized toward the empty site. When the olefin is rotated by 90°, π^*_{CC}

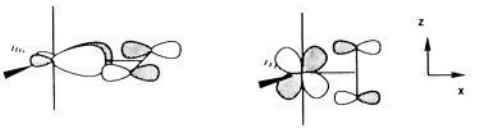

7 8

overlaps with a deeper orbital, *xz*, **8**. The interaction is weaker since the *xz* is further away in energy from π^*_{CC}; in addition, the associated overlap (0.16) is small since the orbital is not hybridized.

The above reasoning needs to be modified when CO ligands are introduced. First π^*_{CO} orbitals lower the energy of *xz* more than that of *xy*, and the lowering is more important for apical CO ligands than for equatorial CO ligands due to better overlap. This effect should have increased the rotation barrier because of a widening of the energy gap between *xy* and *xz*. However, consideration of the overlap of π^*_{CC} with the L_4Ir^+ fragment orbitals drastically modifies this result.

In the case of apical CO, the small overlap between *xz* and π^*_{CC} (when compared to that of *xy* and π^*_{CC}) is partially compensated by the presence of π^*_{CO}s whose carbon contribution overlaps in phase with the olefin π^*_{CC}, when the olefin is perpendicular to the equatorial plane as shown in **9**. No equivalent overlap is present when CO is at the equatorial sites since they are too far from the olefin. Since the interaction between orbitals is pro-

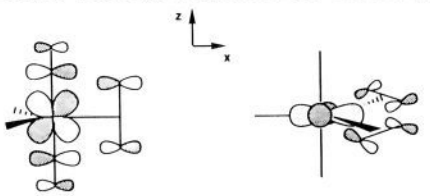

9 10

portional to the square of the overlap, apical CO ligands contribute to a lower olefin rotational barrier by stabilizing the transition state.

Returning to the bis-olefin complex, there is an additional factor in favor of the equatorial conformation. This is illustrated in **10**, looking at the complex in a different set of axes. The *xy* orbital has now become x^2-y^2. **10** shows that the metal orbital overlaps with π^*_{CC} of each ethylene. This creates an in-phase interaction between the two carbons *on different ethylenes*, which contributes to the additional stability of this conformation.

(2) Pseudorotation. Equivalencing the phosphine ligands requires axial/equatorial site exchange. This is usually achieved by a pseudorotation. In Berry pseudorotation, two equatorial ligands become apical, the two apical ligands become equatorial, and one ligand, called the pivot, is unaffected. Thus, in a bis-olefin complex, at least one olefin will become apical in this process. To study such a possibility, we have calculated four conformations, **11**–**14**, of the apical/equatorial bis-olefin complex $Ir(C_2H_4)_2(PH_3)_3^+$. Below each conformation is given the energy in kcal/mol relative to the most stable (diequatorial) conformation.

All of these conformations are high in energy, especially **13** and **14**, where the equatorial olefin is perpendicular to the equatorial plane. The difference in energy between **11** and **13** is approximately that of rotating an olefin in the diequatorial structure. Therefore, bringing one olefin to the apical site does not ease the

(21) Ammeter, J. H.; Bürgi, H.-B.; Thibeault, J. C.; Hoffmann, R. *J. Am. Chem. Soc.* **1978**, *100*, 3686.

(22) (a) For cis π-acceptor ligands, see: Volatron, F.; Eisenstein, O. *J. Am. Chem. Soc.* **1986**, *108*, 2173, and references therein. (b) For trans π-acceptor ligands, see for instance in the case of dialkynes: Birdwhistell, K. R.; Tonker, T. L.; Templeton, J. L. *J. Am. Chem. Soc.* **1987**, *109*, 1401, and references therein. In the case of diolefins: Carmona, E.; Galindo, A.; Marin, J. M.; Gutierrez, E.; Monge, A.; Ruiz, C. *Polyhedron* **1988**, *7*, 1831, and references therein.

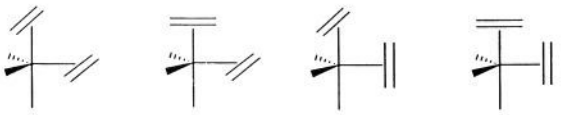

ΔE:	43	34	93	103
	11	12	13	14

rotational barrier. This seems to contradict the finding that π-acceptor ligands facilitate the rotation. In fact, CO and ethylene are very different in that CO offers two π^*_{CO}, whereas ethylene is a single-faced π-acceptor. Only structure **14** will allow a large overlap between the equatorial π^*_{CC} and the xz orbital via the in-phase interaction with the neighboring apical ethylene π^*_{CC} as illustrated in **15**. However, it has been clearly shown that it

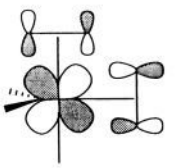

15

is highly unfavorable for a compound bearing two single face π-acceptor ligands to have both π^*_{CC}-accepting orbitals overlapping with the same metal d orbital and leaving the other ones unstabilized.[22] This is the reason for the high energy of conformation **14**.

We thus need only to consider structures **11** and **12**. The reason for their higher energy with respect to the diequatorial conformer results from σ- and π-effects. σ-Effects are not easy to account for. It has been shown that strong σ-donors tend to prefer the apical site.[10] Phosphine (not ethylene) thus prefers the apical site. At the apical site, π^*_{CC} can only interact with energetically remote nonhybridized xz (in **16**) or yz (in **17**), which provides less back bonding than xy as shown in **7**.[23]

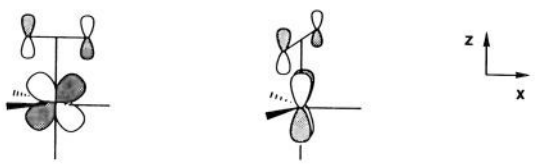

16 17

The replacement of phosphine by CO ligands on the metal makes the pseudorotation considerably easier. When replacing phosphine ligands by CO groups, the structures **11**–**14** are only found 19, 32, 53, 85 kcal/mol higher in energy than the most stable diequatorial conformation. Back bonding to ethylene is diminished, which results in a smaller energy difference between the various conformations. Similar ligand effects are found when calculating intermediate structures on the pseudorotation pathway.

In conclusion, fluxionality is not a property inherent to transition-metal pentacoordination but derives from strong π-acceptor ligands, particularly when there are five identical ligands. Fluxionality in other types of complexes may also be dependent on "spectator ligand" identity.

(3) Isomeric Allene Complexes. Calculations were also done on three isomers of the bis-allene complex with P = PH_3. The relative energies in kcal/mol are shown in Chart II. In agreement with the experimental results, **18** is found to be more stable than **19**, both of them being more stable than the unobserved compound

Chart II

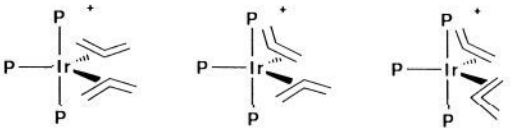

ΔE:	0	1.5	3.2
	18	19	20

20. The analysis of the orbitals of the bis-allene complex reveals that the preference for **18** is due to a smaller four-electron destabilization between the occupied xy metal orbital and the antisymmetric allene combination $\pi_1-\pi_2$. In the ethylene case, such four-electron destabilization is present but cannot be relieved due to the internal symmetry of the ethylene. This is not the case in the present bis-allene complex. The occupied allene π-orbitals are more centered on the terminal than at the central carbon. Taking into consideration the angle between the two coordinated double bonds, it is apparent that the xy orbital overlaps more with the "inside" carbon than "outside" one. As a consequence, minimum four-electron repulsion will be found when the carbon with the smallest density is at the "inside" position, which is **18**. Interconversion between isomers **18** and **19** will, of course, be slow (as observed), following the principles discussed above for olefin rotation in $Ir(C_2H_4)_2(PH_3)_3^+$.

Discussion

Protonation of IrH_3P_3 in CH_2Cl_2 leads to the formation of the dihydrogen complex $IrH_2(H_2)P_3^+$. This formulation allows $IrH_2(H_2)P_3^+$ to avoid d^4 Ir(V) and to achieve a preferred octahedral d^6 configuration. Such a configuration is common to most dihydrogen complexes.

Facile elimination of H_2 is a characteristic reaction of $IrH_4P_3^+$. Rhodes[3] found that when $IrH_4P_3^+$ is placed under a D_2 atmosphere, all hydride ligands are replaced by deuterium. Lewis bases such as CO, THF, and CH_3CN can be used to trap the unsaturated H_2 loss species $IrH_2P_3^+$ forming $IrH_2(L)P_3^+$. $IrH_4P_3^+$ in CH_2Cl_2 thus serves as a convenient source of the reactive, unsaturated hydride species $IrH_2P_3^+$.

Under conditions of excess olefin (ethylene, allene), $IrH_4P_3^+$ loses H_2, binds and reduces 1 equiv of olefin (releasing ethane or propene), and ultimately forms a bis-olefin complex. While the mechanism of reaction with ethylene has been detailed (Scheme I), it was anticipated that cis,bis-olefin complexes might react further by oxidative coupling to form metallacycles.

The coupling of two olefin ligands (eq 7) to form a metallacyclopentane species has been observed on iron[24] and nickel.[25] The

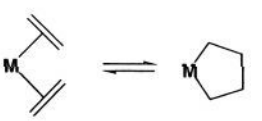

(7)

coupling process in these complexes has been found to be rapidly reversible. Deuterium labeling studies[26] have established the bis-ethylene/metallacycle equilibria for $(PPh_3)_2Ni(C_2H_4)_2$, while the use of an activated olefin and trapping ligand (CO) have led to the isolation and structural characterization[27] of the iron metallacycle, $(CO)_4Fe((CO_2Me)CHCH_2)_2$.

(23) Compounds with apical olefins have been observed. However, in these compounds, cyclic constraints are responsible for this preference. See: Churchill, M. R.; Bezman, S. A. *Inorg. Chem.* **1972**, *11*, 2243. Churchill, M. R.; Lin, K.-K. G. *J. Am. Chem. Soc.* **1974**, *96*, 76. Porta, P.; Powell, H. M.; Mawby, R. J.; Venanzi, L. M. *J. Chem. Soc. A* **1967**, 455.

(24) (a) Weissberger, E.; Laszlo, P. *Acc. Chem. Res.* **1976**, *9*, 209, and references cited therein. (b) Schmid, H.; Naab, P.; Hayakawa, K. *Helv. Chim. Acta* **1978**, *61*, 1427. (c) Grevels, F.-W.; Feldhoff, U.; Leitich, J.; Krüger, C. *J. Organomet. Chem.* **1976**, *118*, 79, and references cited therein.

(25) (a) Grubbs, R. H.; Mitashita, A.; Liu, M.-I.; Burk, P. L. *J. Am. Chem. Soc.* **1977**, *99*, 3863. (b) Grubbs, R. H.; Mitashita, A. *J. Am. Chem. Soc.* **1978**, *100*, 1300.

(26) Grubbs, R. H.; Mitashita, A.; Liu, M.-I.; Burk, P. L. *J. Am. Chem. Soc.* **1978**, *100*, 2418.

(27) Krüger, C.; Tsay, Y.-H. *Cryst. Struct. Commun.* **1976**, *5*, 215.

However, in the case at hand, an attempt to trap[28] or promote ethylene coupling by addition of CH_3CN or MeLi to the bis-ethylene complex $Ir(C_2H_4)_2P_3^+$ only led to rapid displacement of ethylene. This led to the discovery of reversible ethylene dissociation as a characteristic reaction of $Ir(C_2H_4)_2P_3^+$.

The coupling of activated olefins such as allene has been found to be a much more facile process.[29] With allene, coupling most often occurs[30] at the two central carbons to give metallacyclopentane compounds containing exocyclic methylenes.[31]

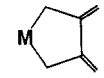

M = Rh, Ir, Ni

When allene is reacted with $IrH_4P_3^+$, propene and a product having the molecular formula $Ir(C_3H_4)_2P_3^+$ are formed. While ^{31}P, ^1H NMR were insufficient to distinguish between a bis-allene complex and a coupled metallacycle product, we anticipated that it might be possible to distinguish these based on ^{13}C chemical shifts and C–H coupling constants.[32] If the metallocyclic complex was formed, chemical shifts consistent with a metal bound sp^3 hybridized carbon would be expected. Such signals are usually observed at high field (<30 ppm) and exhibit C–H couplings of 110–140 Hz. A bis-allene complex, like other olefin complexes, would be expected to have a ^{13}C chemical shift for the metal bound sp^2 carbon in the 20–80 ppm region. A C–H coupling constant on the order of 150–170 Hz would accompany this ^{13}C chemical shift. The ^{13}C NMR data for $Ir(C_3H_4)_2P_3^+$ proves ambiguous, however. The ^{13}C chemical shifts at 103.3 and 149.2 ppm are consistent[32b] with an unbound or exocyclic sp^2 carbon and a quaternary carbon, respectively. The remaining ^{13}C resonance at 7.27 ppm, which couples to one phosphine ligand (J_{C-P} = 4.5 Hz) encourages interpretation as belonging to a metal bound sp^3 carbon. This resonance, however, possesses a C–H coupling constant of 158 Hz, clearly diagnostic of an sp^2 hybridized carbon. In light of the structural study, it would appear that the value of the C–H coupling constant is a more reliable indicator of the nature of the allene product than is the ^{13}C chemical shift.

We next address the question of what it is about the mechanism of formation of $Ir(C_3H_4)_2P_3^+$ that causes initial formation of an unstable isomer (i.e., the kinetic product **6c**). The hypothesis

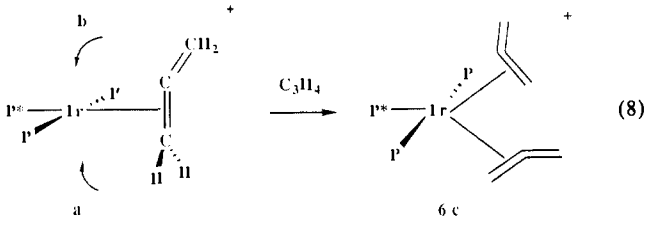

(8)

that it forms from $Ir(C_3H_4)P_3^+$ (in which the allene axis lies perpendicular to the planar IrP_3 array) explains this naturally, assuming the second allene approaches (eq 8) from the "a" side with the pendant double bond oriented away from the bulkiest group, P*. The symmetrical bis-allene complex **6a** is the thermodynamic product in this reaction, resulting from the isomerization of an initial unsymmetrical bis-allene complex **6c**. This isomerization could be achieved by an intramolecular migration of one of the η^2-allene ligands similar to that proposed for $(CO)_4Fe(Me_2C_3Me_2)$.[33] This involves moving iridium between the two C=C bonds of one allene. Interestingly, while this process is rapid and reversible for $(CO)_4Fe(Me_2C_3Me_2)$, it is slow for **6**. This demonstrates again the influence of the strong π-acceptor CO in reducing the activation energy to rearrangement.

That $IrH_4P_3^+$ is an effective hydrogenation catalyst is not altogether surprising since the clearly related complex, $IrH_2S_2P_2^+$ (S = solvent, P = PPh_3), also hydrogenates olefins catalytically. Generated in situ from $[(COD)IrP_2]BF_4$ and H_2, the $IrH_2S_2P_2^+$ system[15,34] shares some common intermediates and characteristics with the $IrH_4P_3^+$ system reported here. Both systems contain spectroscopically observable hydrido–olefin complexes as well as bis-olefin species. However, the presence of an extra nondissociating phosphine ligand in the $IrH_4P_3^+$ system raises the possibility of superior catalytic properties. For instance, in the $IrH_2S_2P_2^+$ system, irreversible catalyst deactivation to the hydride-bridged dimer, $[Ir_2H_2(\mu\text{-}H)_3L_4]BF_4$, occurs competitively with olefin hydrogenation. This result becomes even more pronounced at low olefin concentrations. With $IrH_4P_3^+$, dimer formation is never observed; the added steric requirements associated with three phosphine ligands must prohibit dimerization under these conditions. It may also be that three phosphine ligands will exert more steric control over any reaction which could proceed via primary or secondary alkyl complexes (e.g., olefin isomerization). We will report on attempts to extend this principle to a tetrakis-phosphine complex in a separate publication.

Acknowledgment. We thank the U.S. NSF (Grant No. 8707055) for financial support and Johnson-Matthey Co. for material support. O.E. acknowledges the Indiana University Institute for Advanced Study for a fellowship. The Laboratoire de Chimie Théorique is associated with the CNRS (UA 506) and is a member of ICMO and IPCM. We also acknowledge CNRS and NSF for an international travel grant.

Supplementary Material Available: Tables of anisotropic thermal parameters for $[Ir(C_2H_4)_2(PMe_2Ph)_3]BF_4 \cdot 0.5H_2O$ and $[Ir(C_3H_4)_2(PMe_2Ph)_3]BF_4$ (3 pages); tables of observed and calculated structure factors (26 pages). Ordering information is given on any current masthead page.

(28) Stockis, A.; Hoffmann, R. *J. Am. Chem. Soc.* **1980**, *102*, 2952.
(29) Collman, J. P.; Hegedus, L. S.; Norton, J. R.; Finke, R. G. *Principles and Applications of Organotransition Metal Chemistry*; 1987; University Science Books: p 498.
(30) Other types of allene coupling are also known, see: (a) Schmidt, J. R.; Duggan, D. M. *Inorg. Chem.* **1981**, *20*, 318. (b) Lewandos, G. S.; Doherty, N. M.; Knox, S. A. R.; MacPherson, K. A.; Orpen, A. G. *Polyhedron* **1988**, *7*, 837.
(31) (a) Diversi, P.; Ingrosso, G.; Immirzi, A.; Zoccki, M. J. *J. Organomet. Chem.* **1976**, *104*, C1. (b) Ingrosso, G.; Porri, L.; Pantini, G.; Racanelli, P. *J. Organomet. Chem.* **1975**, *84*, 75. (c) Ingrosso, G.; Immirzi, A.; Porri, L. *J. Organomet. Chem.* **1973**, *60*, C35. (d) Jolly, P. W.; Krüger, C.; Salz, R.; Sekutowski, J. C. *J. Organomet. Chem.* **1979**, *165*, C39.
(32) (a) Mann, B. E. *Adv. Organomet. Chem.* **1974**, *10*, 135. (b) Jolly, P. W.; Mynott, R. *Adv. Organomet. Chem.* **1981**, *19*, 257.
(33) Ben-Shoshan, R.; Pettit, R. *J. Am. Chem. Soc.* **1967**, *89*, 2231.
(34) Crabtree, R. H.; Mellea, M. F.; Mihelcic, J. M.; Quirk, J. M. *J. Am. Chem. Soc.* **1982**, *104*, 107.